Title

Focal Adhesion Kinase (FAK) Nuclear Localization Enhances Cisplatin Chemotherapy Resistance in Ovarian Carcer

Author

Zhang, Yichi

Publication Date

2023

Peer reviewed|Thesis/dissertation

UNIVERSITY OF CALIFORNIA SAN DIEGO

Focal Adhesion Kinase (FAK) Nuclear Localization Enhances Cisplatin Chemotherapy Resistance in Ovarian Cancer

A Thesis submitted in partial satisfaction of the requirements

for the degree Master of Science

in

Biology

by

Yichi Zhang

Committee in charge:

Professor David D. Schlaepfer, Chair

Professor Dong-Er Zhang, Co-Chair

Professor Heidi Cook-Anderson,

Professor Dwayne G. Stupack,

The Thesis of Yichi Zhang is approved, and it is acceptable in quality and form for publication on microfilm and electronically.

University of California San Diego

2023

DEDICATION

I would like to dedicate this thesis to my family and friends. Thanks for their unconditional support. I’m grateful for having them in my life.

TABLE OF CONTENTS

LIST OF ABBREVIATIONS

FACS: fluorescence-activated cell sorting

FAK: Focal Adhesion Kinase

FERM: band 4.1, ezrin, radixin, and moesin homology

GFP: green fluorescent protein

HGSOC: high grade serous ovarian cancer

KMF: KRas, Myc, and FAK ovarian tumor cells

KO: knockout

NLS: N-terminal domain-containing point mutations (R177A R178A)

WT: wildtype

ACKNOWLEDGEMENTS

I would like to first thank Dr. David Schlaepfer for providing me the support over the last two and a half years. I am grateful for the opportunities and guidance he has provided to me throughout this process.

I also want to thank Dr. Marjaana Ojalill for all the help she provided. Her support helped me went through the tough moments.

Lastly, I would like to thank all the members of the Schlaepfer lab and Stupack lab. I wish them the best of luck and success in the future.

ABSTRACT OF THE THESIS

Focal Adhesion Kinase (FAK) Nuclear Localization Enhances Cisplatin Chemotherapy Resistance in Ovarian Cancer

by

Yichi Zhang

Master of Science in Biology

University of California San Diego, 2023

Professor David D. Schlaepfer, Chair

Ovarian cancer is one of the deadliest cancers affecting women worldwide. Platinum with paclitaxel chemotherapy after surgery is standard of care. However, ~80% of patients will recur and eventually develop chemotherapy resistance with few approved treatment options. In both high grade serous ovarian cancer (HGSOC) and murine models of ovarian cancer, elevated focal adhesion kinase (FAK) expression is common and increased FAK tyrosine phosphorylation has been linked to adaptive chemotherapy resistance. Herein, I present results that cisplatin but not paclitaxel chemotherapy increases FAK tyrosine phosphorylation and nuclear accumulation as evaluated by biochemical cell fractionation, immunofluorescent cell staining, and immunoblotting. To create a model to test FAK nuclear function, FAK knockout ovarian tumor cells were stably reconstituted with green-fluorescent fusion proteins of FAK wildtype (WT) or a N-terminal domain-containing point mutations (R177A R178A, NLS$^-$) of FAK that prevents nuclear localization. Both FAK-WT and FAK-NLS$^-$ grow equivalently in cell culture and 20 μM cisplatin for 12 hours (below IC50 concentration for cell death) triggered FAK-WT but not FAK-NLS$^-$ nuclear accumulation with increased apoptosis occurring in FAK-NLS$^-$ compared to FAK-WT cells. FAK-WT promoted cisplatin resistance compared to FAK-NLS$^-$ whereas sensitivity to paclitaxel chemotherapy was unchanged. Notably, FAK-WT and FAK-NLS$^-$ ovarian tumor cells grew equivalently upon orthotopic injection in mice whereas cisplatin treatment (2 mg/kg, weekly) significantly prevented FAK-NLS$^-$ tumor growth compared to FAK-WT tumors. These results show that intrinsic FAK nuclear localization within ovarian tumor cells is associated with resistance to cisplatin-mediated cell death *in vitro* and *in vivo*. Ongoing studies are focused on unraveling cell survival signal(s) associated with nuclear FAK.

INTRODUCTION

Ovarian cancer is a common and deadly female cancer worldwide, and it is the most lethal gynecologic malignancy in the United States (Siegel et al. 2023). High-grade serous ovarian carcinoma (HGSOC) is the most common epithelial ovarian cancer (Matulonis et al. 2016) and standard-of-care treatment for HGSOC involves cytoreductive surgery followed by cisplatin/carboplatin (DNA damage generation) with paclitaxel (microtubule stabilizing drug) chemotherapy (Kim et al. 2018). Although most patients initially respond to primary chemotherapy (Agarwal and Kaye 2003), approximately 80% of HGSOC patients will exhibit tumor recurrence within 5 years, will progressively develop chemotherapy resistance after retreatment, and will eventually succumb to this disease (Bowtell et al. 2015). As there are few approved treatment options for platinum chemotherapy resistant HGSOC, it is urgent to understand the underlying mechanism of cisplatin drug resistance and explore for new therapy options for ovarian cancer patients.

Focal Adhesion Kinase (FAK) is a 120 kDa cytoplasmic protein-tyrosine kinase best known for promoting normal and tumor cell movement (Mitra, Hanson, and Schlaepfer 2005). The FAK (*PTK2*) gene undergoes gains and amplification in breast, uterine, cervical, and ovarian tumors (Kaveh et al. 2016) and elevated FAK mRNA and protein levels in HGSOC are associated with tumor progression and a poor prognosis (Murphy et al. 2020). Most research about FAK function is focused on its scaffolding and signaling roles in the cytoplasm or at cell adhesions (Sulzmaier, Jean, and Schlaepfer 2014) and FAK can be recruited to the cell membrane in response to growth factor stimulation of cells (Chen et al. 2012). However, in

response to stress stimuli, FAK can translocate to the cell nucleus where it has been proposed to promote cell survival during mouse development in the regulation of p53 tumor suppressor protein levels by facilitating p53 ubiquitination (Lim et al. 2008). Interestingly, nuclear-localized FAK can modulate inflammatory gene expression in a kinase-independent manner in endothelial cells (Lim et al. 2012) or via proposed interactions with transcription factor complexes in a kinase-dependent manner in carcinoma cells (Serrels et al. 2015; Canel et al. 2017). Immunohistochemical staining of tumors with antibodies to FAK that is phosphorylated at tyrosine-397 (pY397) reveals expression of FAK pY397 in the nuclei of breast and ovarian carcinomas (Tancioni et al. 2015; Tancioni et al. 2014) and nuclear FAK is associated with a poor prognosis in human colorectal cancer (Albasri et al. 2014).

FAK protein is comprised of N-terminal FERM (band 4.1, ezrin, radixin, and moesin homology), central catalytic kinase region, proline-rich domains that serve as binding sites for other signaling proteins, and a C-terminal focal adhesion targeting domain (Schlaepfer, Hauck, and Sieg 1999). Protein crystal structure analyses reveal a three-lobed FAK FERM domain (Ceccarelli et al. 2006) with a nuclear localization sequence (NLS) comprised of surface-exposed basic amino acids within the F2 lobe of the FAK FERM domain (Lim et al. 2008). What remains unknown are the molecular mechanism(s) regulating FAK nuclear accumulation in cells that can also occur in association with murine keratinocyte transformation into squamous cell carcinoma (Serrels et al. 2015).

Previous studies of FAK function in ovarian cancer showed that FAK silencing augmented docetaxel-mediated apoptosis (Halder et al. 2005), that FAK signaling contributed to paclitaxel resistance (Kang et al. 2013), and that nanoparticles containing paclitaxel and FAK

siRNA could overcome induced chemotherapy resistance in mouse models (Byeon et al. 2018). However, a Phase IB trial of paclitaxel and a small molecular inhibitor of FAK catalytic activity found only limited combinatorial clinical activity in non-selected HGSOC patients (Patel et al. 2014). Interestingly, in an *in vivo* evolved murine model of ovarian cancer, spontaneous genomic copy number gains in Kras, Myc, and FAK genes (termed KMF cells) were associated with enhanced tumor stem cell-like properties (Diaz Osterman et al. 2019). FAK expression and activity were linked to adhesion-independent cell growth and resistance to cisplatin-mediated cell cytotoxicity. Transcriptomic comparisons across FAK knockout and FAK reconstituted KMF cells identified common targets, elevated in HGSOC, that were regulated by FAK including pluripotency and DNA repair genes (Diaz Osterman et al. 2019).

As platinum-resistant KMF three dimensional tumorsphere growth was dependent on FAK expression and activity (Diaz Osterman et al. 2019), we sought to test whether cisplatin stress on ovarian tumor cells could alter FAK cytoplasmic-nuclear accumulation and whether nuclear FAK contributes to cisplatin chemotherapy resistance. By comparing FAK knockout KMF cells reconstituted with green fluorescent protein (GFP) fusions with wildtype or an NLS-deficient (NLS$^-$) FAK point mutant in vitro by biochemical cell fractionation, immunofluorescent cell staining, and immunoblotting cell lysates, we find that cisplatin treatment enhances FAK nuclear accumulation and is associated with resistance to cisplatin-mediated cell apoptosis. These findings parallel nuclear FAK accumulation in HGSOC cells treated with cisplatin and the increased sensitivity of FAK NLS$^-$ KMF cells to cisplatin when grown as tumors in mice. As a Phase I clinical trial is testing the safety of a small molecule FAK inhibitor, carboplatin, and paclitaxel in recurrent platinum resistant HGSOC at the UCSD

Moores Cancer Center (NCT03287271), our results provide additional insights into the importance of nuclear FAK in promoting cisplatin chemotherapy resistance.

RESULTS

Nuclear FAK accumulation occurs upon cisplatin treatment of ovarian tumor cells

To study the role of nuclear FAK, we used a spontaneously derived murine ovarian tumor model (Ward et al. 2013) with gains in KRas, Myc, and FAK genes termed KMF cells (Diaz Osterman et al. 2019). Endogenous FAK expression was inactivated in KMF cells using CRISPR-Cas9, DNA sequencing validated target site inactivation, immunoblotting was used to verify loss of FAK protein expression, and exon sequencing was performed that confirmed no potential oncogenic mutations in KMF clone KT13 FAK knockout (KO) cells (Diaz Osterman et al. 2019). Herein, KMF FAK-KO cells were transduced with recombinant lentivirus to express N-terminal GFP fusion proteins of FAK wildtype (WT) or a FAK NLS$^-$ mutant that contains point mutations at residues R177 and R178 to alanine (Fig. 1A). Pooled re-expressing cells were enriched and sorted for GFP expression by FACS (fluorescence-activated cell sorting). Immunoblotting whole cell lysates with antibodies to GFP and FAK phosphorylated at the Y-397 site (pY397), used as an indirect marker of FAK activity (Dawson et al. 2021), revealed equal FAK-WT and FAK-NLS$^-$ expression with FAK-KO lysates as control (Fig. 1A). This FAK-NLS$^-$ mutant exhibits slightly lower pY397 FAK levels compared to FAK-WT (Fig. 1A). Previous published studies using additional FAK FERM point mutations to disrupt FAK NLS targeting show a loss of pY397 FAK phosphorylation (Dunty et al. 2004; Serrels et al. 2015) whereas mutations in nearby FAK FERM residues Y-180 and M-183 enhance pY397 FAK phosphorylation (Lietha et al. 2007; Cai et al. 2008). GFP-FAK-NLS$^-$ used herein has been shown to control vascular smooth muscle proliferation (Jeong et al. 2019).

To visualize whether cisplatin chemotherapy stress can alter FAK distribution, FAK-WT and FAK-NLS$^-$ KMF cells were plated on glass coverslips and imaged by laser scanning confocal microscopy under control (DMSO) or cisplatin (20 μM) addition for 12 hr. Shown are representative images of Z planes for nuclear (stained with DAPI), cell midline (GFP-FAK), and a merged image of both (Fig. 1B). Under control conditions, cytoplasmic distribution was equivalent for FAK-WT and FAK-NLS$^-$ with only a weak nuclear signal (Fig. 1B). However, upon cisplatin stimulation, FAK-WT exhibited nuclear accumulation whereas FAK-NLS$^-$ remained in the cell cytoplasm (Fig. 1B). Non-denaturing biochemical fractionation of FAK-WT and FAK-NLS$^-$ cell lysates into nuclear and cytoplasmic fractions followed by immunoblotting confirmed increased FAK-WT nuclear accumulation within 12 hr. and remaining in the nucleus at 24 hr. (Fig. 1C). FAK-NLS$^-$ remained in the cytoplasm fraction wherein levels of both FAK-WT and FAK-NLS$^-$ were equivalent (Fig. 1C).

To determine if endogenous ovarian tumor expressed FAK undergoes nuclear accumulation upon cisplatin stress, HGSOC cell lines OVCAR3 and OVCAR4 were evaluated for cisplatin cytotoxicity *in vitro* and found to be more sensitive than KMF FAK-WT cells (Fig. 1D and Fig. 2A). Thus, 1 μM cisplatin or DMSO were added to cultures of OVCAR3 or OVCAR4 cells for 12 hr followed by cell lysate separation into nuclear of cytoplasmic fractions (Fig. 1E). Interestingly, the higher FAK expressing and more cisplatin resistant OVCAR4 cells showed strong cisplatin stimulated FAK nuclear accumulation and nuclear pY397 FAK tyrosine phosphorylation compared to weak FAK nuclear distribution in OVCAR3 cells (Fig. 1E). Taken

together, these results show that cisplatin stress can trigger FAK nuclear accumulation and pY397 tyrosine phosphorylation murine and human ovarian tumor cells which is disrupted by point mutations (R177A R178A) in the FAK FERM NLS targeting motif.

FAK nuclear localization promotes cell survival in response to cisplatin

To evaluate quantitatively the cellular survival response to cisplatin addition, KMF FAK-KO, FAK-WT, and FAK-NLS$^-$ cells were evaluated for viability after 48 hr in increasing concentrations of cisplatin (Fig. 2A). Half-maximal inhibitory concentrations (IC50) were determined: 20.1 +/- 4.5 µM, 29.3 +/- 2.4 µM, and 40.2 +/- 3.9 µM cisplatin for FAK-KO, FAK-NLS$^-$ cells, and FAK-WT, respectively. The difference between FAK-WT and FAK-NLS$^-$ resistance to cisplatin was significant and this finding also extended to FAK-KO OVCAR3 cells re-expressing GFP-FAK-WT or GFP-FAK-NLS$^-$ where FAK WT supported greater cisplatin resistance (Fig. 2A). Interestingly, both KMF FAK-WT and KMF FAK-NLS$^-$ cells showed equal resistance to paclitaxel after 48 hr. (Fig. 2A) and paclitaxel did not promote detectable FAK nuclear accumulation (data not shown). Together, these results support the notion that FAK may respond differently to chemotherapy stress as neither cisplatin nor paclitaxel are known to directly bind to FAK. Moreover, these results show that FAK nuclear localization is associated with increased cell survival to cisplatin stress.

To measure proliferation and survival differences in culture, equal numbers of KMF FAK-WT and KMF FAK-NLS$^-$ cells were cultured in growth media containing increasing amounts of cisplatin for 10 days and cell colonies were visualized by crystal violet staining (Fig. 2B). Dye quantitation revealed no differences under control (DMSO) conditions and

significantly fewer colonies formed by FAK-NLS⁻ compared to FAK-WT in the presence of 1 μM cisplatin (Fig. 2C). These supports the notion that nuclear FAK provided a growth and survival advantage in the presence of cisplatin. Cell survival signaling was analyzed by treating FAK-WT and FAK-NLS⁻ cells with cisplatin (20 μM, 12 hr.) and performing immunoblotting with antibodies to BAX (pro-death), Bcl2 (pro-survival), cleaved caspase 3 (apoptosis marker) and β-tubulin as a loading control (Fig. 2D). After cisplatin treatment, slightly higher levels of BAX and cleaved caspase 3 with lower levels of Bcl2 were present in FAK-NLS⁻ cells compared to FAK-WT (Fig. 2D). Additionally, when comparing human OVCAR10 ovarian tumor cells to *in vitro*-derived cisplatin resistant OVCAR10-CP cells (Diaz Osterman et al. 2019), sub-cytotoxic levels of cisplatin treatment in culture followed by nuclear-cytoplasmic fractionation revealed increased FAK nuclear localization in OVCAR10-CP cells and increased nuclear FAK pY397 phosphorylation after cisplatin stimulation (Fig. 2E). Taken together, we conclude that stimulated FAK nuclear localization and tyrosine phosphorylation is a conserved pro-survival response to cisplatin stress in ovarian tumor cells.

Differential KMF growth of FAK-WT and FAK-NLS⁻ cells as tumors in mice with cisplatin treatment

To test the connection between FAK nuclear accumulation and growth as tumors in mice, KMF GFP-FAK-WT and GFP-FAK-NLS⁻ cells were intraperitoneal injected into C57Bl6 mice as an orthotopic ascites tumor model (Diaz Osterman et al. 2019). Mice were randomized into four experimental groups at Day 5 after *in situ* tumor cell detection was quantified by luciferase

based IVIS imaging (Figs. 3A and B). FAK-WT and FAK-NLS tumor bearing control mice received three saline instead of cisplatin (4 mg/kg) injections on Days 10, 17, and 24 and all mice were IVIS imaged as indicated and mice euthanized at Day 31 (Fig. 3A). Plotting mean IVIS bioluminescence over time revealed that FAK-WT and FAK-NLS cells grew equivalently as tumors (Fig. 3B). Weekly cisplatin treatment reduced both FAK-WT and FAK-NLS tumor growth compared to saline control and FAK-NLS tumor burden was significantly less than FAK-WT at Day 31 (Fig. 3B).

To test whether differences in KMF FAK-WT and FAK-NLS$^-$ tumor growth may be revealed using less cisplatin (2 mg/kg) over a longer experimental time period, a similar experiment was repeated as outlined in the schematic (Fig. 3C) that incorporated six cisplatin administrations to mice over a 49-day period. Representative IVIS imaging at Day 45 showed clear differences in tumor burden between FAK-WT and FAK-NLS$^-$ tumors (Fig. 3D). Plotting mean IVIS bioluminescence over time revealed significantly greater FAK-WT tumor growth compared to FAK-NLS$^-$ (Fig. 3E). Isolation and enumeration of cells collected from a peritoneal wash of tumor bearing mice at Day 49 confirmed significantly more cells recovered in FAK-WT versus FAK-NLS$^-$ tumor bearing mice (Fig. 3F). Taken together, these results support the conclusion that nuclear FAK enhances cisplatin chemotherapy resistance.

DISCUSSION

Our research showed that cisplatin chemotherapy treatment triggered wild-type (WT) FAK (Focal Adhesion Kinase) nuclear accumulation, and this enhanced ovarian tumor cells survival to cisplatin chemotherapy *in vitro* and *in vivo*. In our research, we utilized KMF FAK knockout cells re-expressed with either WT FAK or NLS-FAK construct. The NLS-FAK constructs involved two mutations in the F2 FERM domain of FAK, specifically changing R177 and R178 into alanine. Based on nuclear/cytoplasmic fractionation and immunofluorescent staining, we observed that FAK NLS$^-$ effectively prevented FAK nuclear translocations under chemotherapy stimulation. By comparing the two constructs, we also concluded that WT FAK accumulated in the nucleus after cisplatin treatment. Our study revealed that this phenomenon is not limited to the KMF cell line but extends to OVCAR cell lines as well. Through testing the IC50 value, we identified a correlation between increasing cisplatin resistance and the existence of nuclear FAK translocation after cisplatin treatment. Importantly, this survival relationship did not manifest in all types of chemotherapy, as no IC50 difference was observed between FAK-WT and FAK NLS$^-$ to paclitaxel. Subsequently, we employed biofractionation and cell colony assays to determine that nuclear FAK plays a role in increasing cell survival and preventing cisplatin-induced apoptosis levels under cisplatin treatment, thereby enhancing cisplatin resistance. This finding was further validated when FAK-WT and FAK NLS$^-$ cells were grown as tumors in mice. We observed a similar growth pattern between FAK WT and FAK NLS$^-$ in non-treatment groups, and as the mice received different dosages of cisplatin weekly, mice injected with FAK NLS$^-$ cells exhibited a slowed growth rate compared to those injected with WT FAK.

Thus, our research has opened a new perspective on the role of nuclear FAK. Recent studies have reported that the nuclear expression of FAK is related to p53 regulation (Lim et al. 2008), immune escape (Serrels et al. 2015), and cell cycle (Jeong et al. 2022). In our study, we identified a brand-new role for nuclear FAK in connection with cisplatin resistance and observed its accumulation under cisplatin stimulation.

Our result support a promising prospect for the improved treatment of ovarian patients. FAK overexpression is commonly observed in ovarian cancer patients (Xu et al. 2017), and FAK activity has been demonstrated to be associated with both the progression of ovarian cancer and resistance to chemotherapy (Diaz Osterman et al. 2019). Given the high recurrence rate experienced by ovarian cancer patients due to the development of chemotherapy resistance, we directed our focus toward understanding the relationship between FAK mechanisms and cisplatin chemotherapy resistance. Our conclusion indicates that nuclear FAK expression plays a potential role in the development of resistance. In light of our findings, our work underscores the involvement of nuclear FAK in cisplatin chemotherapy resistance and proposes potential therapeutic options for treating chemotherapy-resistant patients with high-grade serous ovarian cancer (HGSOC). Considering the availability of multiple clinically approved FAK inhibitors, our results illustrate a plausible approach for future medication choices.

Ongoing research is focused on what exact underlying mechanism nuclear FAK is playing in order to cause cisplatin resistance to happen. Cisplatin activation has been known to be related with MAPK pathway activation (Pereira et al. 2013) and phosphatase DUSP1 expression changes (Kang et al. 2016). Thus, we are now focusing on investigating if nuclear FAK expression modulates MAPK activation and DUSP1 function. Future studies will be

needed to further elucidate the mechanisms underlying the involvement of nuclear FAK in cisplatin chemotherapy resistance, and testing therapy agents that block nuclear FAK could be a viable strategy for eliminating cisplatin chemotherapy resistance and improving survival expectations in patients. We propose performing in vivo experiment with combination of FAK inhibitor and chemotherapy and compare if the constructs would still lead to a different growing pattern. This will give us a better understanding on what changes have been occurred after the accumulation of nuclear FAK.

Nonetheless, the results of this study provide a strong foundation for further investigation of the role of nuclear FAK in ovarian cancer biology and treatment. Studying nuclear FAK has significant implications for the development of new therapeutic strategies for ovarian cancer treatment. Targeting nuclear FAK could represent a promising approach for overcoming chemotherapy resistance and improving the life expectancy of patients.

Figure 1. FAK FERM dependent nuclear translocation within 12 hrs. of sub-cytotoxic cisplatin stress in ovarian tumor cells.A) Schematic of GFP-FAK with a GFP connected to the FAK n-terminus, followed by FAK FERM containing arginine (R) residues comprising a nuclear localization (NLS) motif, and mutation of residues R177 and R178 to alanine disrupts FAK nuclear targeting (termed NLS$^-$). FAK tyrosine-397 (Y-397) is a major auto-phosphorylation site and indirect measure of FAK activity. FAK FAT, focal adhesion targeting domain. GFP-FAK WT (wildtype) and GFP-FAK-NLS$^-$ were expressed in KRas, Myc, and FAK amplified (KMF) ovarian tumor cells selected previously by CRISPR-Cas9 to delete endogenous FAK expression (FAK KO) (Diaz Osterman et al. 2019). Immunoblotting with antibody to pY397 FAK, GFP-FAK, and actin as a loading control was performed on cell lysates from KMF FAK KO cells and pooled populations of GFP-FAK WT or GFP-FAK-NLS$^-$ stably expressing cells. **B**) Laser scanning confocal imaging was obtained from control (DMSO) or cisplatin-treated (20 μM, 12 hr) GFP-FAK-WT (FAK-WT) or GFP-FAK-NLS$^-$ (FAK NLS$^-$) KMF cells growing on glass coverslips. Shown are representative images with nuclei was visualized by DAPI, intrinsic fluorescence of GFP-FAK (images shown at midline of Z-stack), and a merged imaged. Scale bar is 10 μm. **C**) Immunoblotting of nuclear and cytoplasmic biochemical cell fractionation of FAK-WT (WT) or FAK-NLS- (NLS$^-$) expressing KMF cells at 0, 12, and 24 hr after cisplatin (20 μM) stimulation. Immunoblotting was used to determine GFP-FAK levels in the nuclear (anti histone H3) or cytoplasmic fraction (anti β-tubulin) with control immunoblotting revealing cellular fractionation purity. **D**) Human OVCAR3 and OVCAR4 ovarian tumor cells were evaluated for cisplatin toxicity after 24 hr by Alamar Blue staining and spectroscopy. Show is cell viability (%) versus cisplatin concentration (log_{10}) and points are means of triplicate samples (N=1 independent experiment). **D**) Immunoblotting of nuclear and cytoplasmic cell fractions of OVCAR3 and OVCAR4 cell lysates with anti-FAK pY397, total FAK, β-tubulin, and histone H3. Cells were (1 μM) or DMSO (control) for 12 hr.

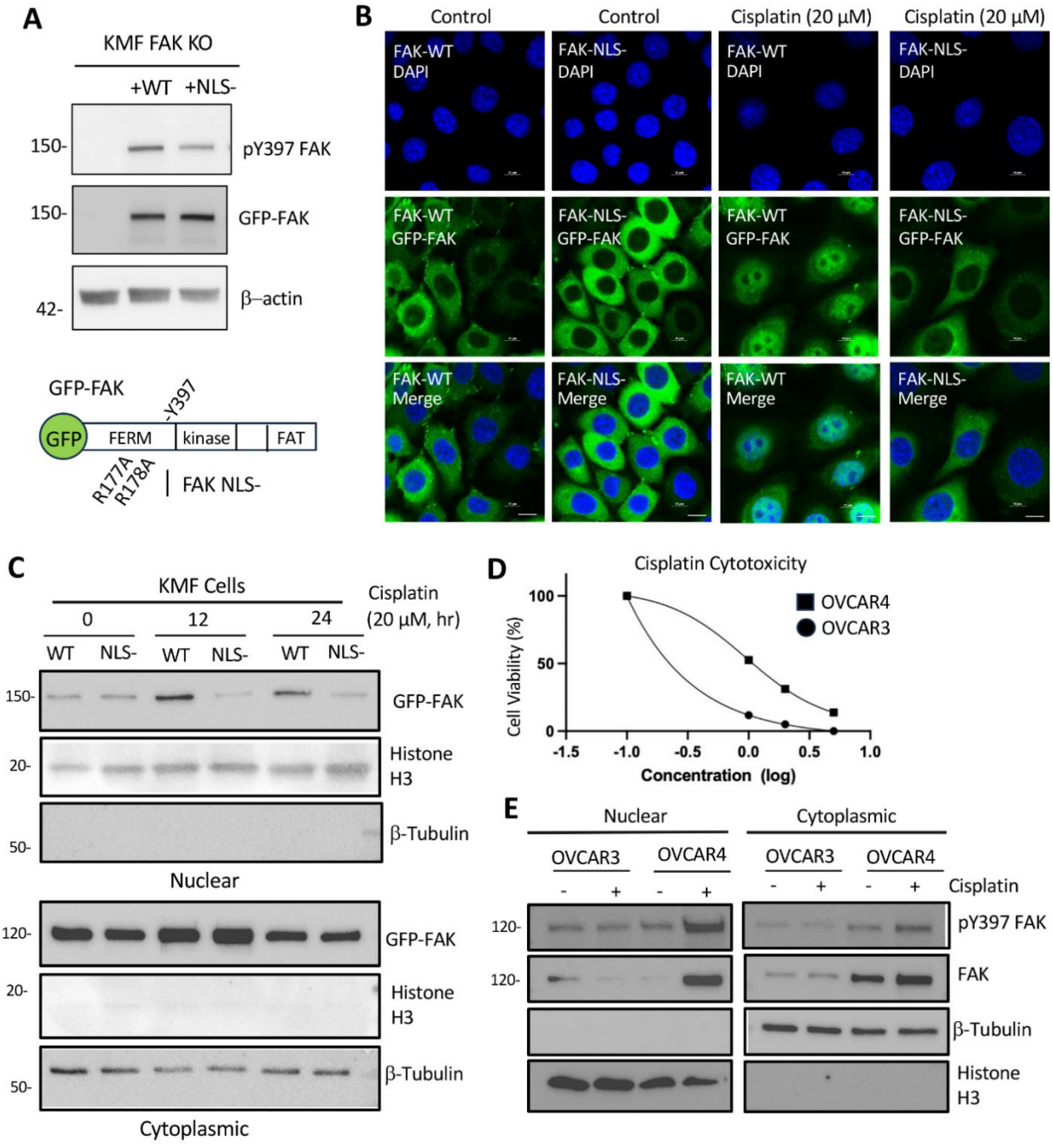

Zhang, Figure 1

Figure 2. Cisplatin-stimulated FAK nuclear localization in ovarian tumor cells is associated with enhanced cell survival. A) Murine KMF-FAK-KO, FAK-NLS$^-$, and FAK-WT cells or human FAK knockout OVCAR3 cells expressing GFP-FAK-WT or GFP-FAK-NLS$^-$ were evaluated for cisplatin toxicity after 48 hr by Alamar blue staining and spectroscopy. Show is cell viability (%) versus cisplatin concentration (log_{10}) and points are means of triplicate samples +/- standard deviation (SD) (n=3 independent experiments). IC50 values for cisplatin or paclitaxel were calculated using Prism 8.0 software. **B**) Colony forming assays were performed with KMF FAK-WT and FAK-NLS$^-$ cells in the presence of increasing concentrations (0, 1, 10 μM) of cisplatin for 10 days. Representative images of crystal violet-stained cell culture plates with increase staining associated with increased cell density. **C**) Image quantitation of KMF FAK-WT (blue bars) and FAK-NLS$^-$ (red bars) colony formation. Values are means from three independent experiments with triplicate points +/-SD, **** $p<0.001$ by one-way ANOVA with Tukey's multiple comparison test. **D**) Increasing BAX and decreased Bcl2 upon cisplatin stimulation in KMF FAK-NLS$^-$ compared to FAK-WT after 12 h cisplatin (20 μM) addition reveals elevated cell apoptotic marker changes. Immunoblotting whole cell lysates from control or cisplatin-stimulation antibodies to BAX, Bcl2, cleaved caspase 3, and β-tubulin as a protein loading control. **E**) Human OVCAR-10 (OV10), and cisplatin-resistant OVCAR-10 CP (OV10-CP) ovarian tumor cells were treated with vehicle (DMSO) control or cisplatin (5 μM) for 12 hrs and cell lysates fractionated in nuclear or cytoplasmic cell fractions and then analyzed by total FAK, pY397 FAK, histone H3, or β-tubulin immunoblotting.

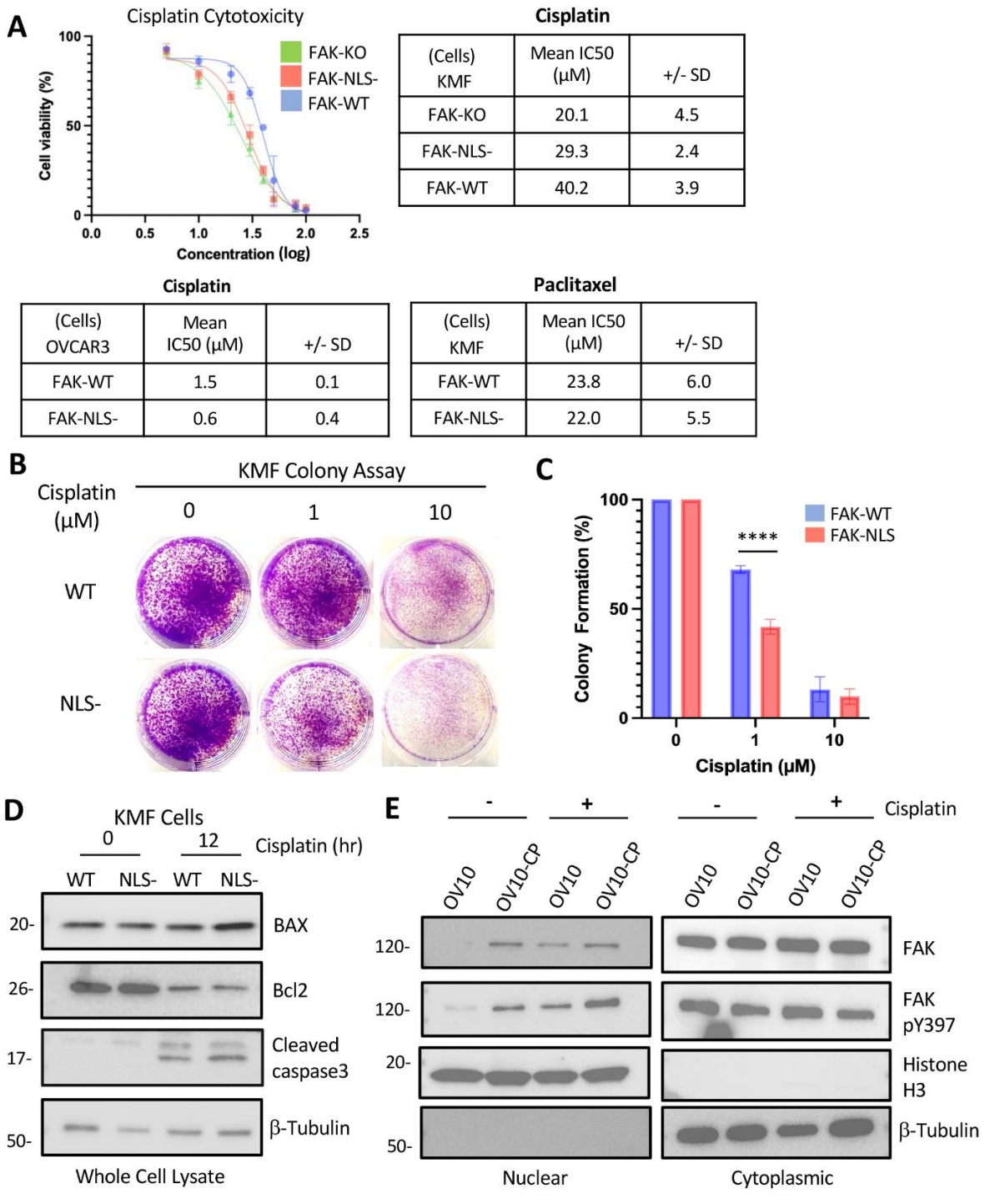

Zhang, Figure 2

Figure 3. Nuclear FAK promotes mouse ovarian tumor resistance to cisplatin chemotherapy. A) Experimental schematic: 7.5 million luciferase-expressing KMF FAK-WT or FAK-NLS$^-$ cells were intraperitoneal (IP) injected with Matrigel-saline into syngeneic C57Bl6 mice (Day 0). Tumor cell levels were measured at Day 5 by an IVIS small animal imaging system (PerkenElmer) and mice were randomized into experimental groups (n=8 each). Mice were administered saline or cisplatin (CP, 4 mg/kg) on Day 10, 17, and 24. Mice were IVIS imaged for tumor cell burden on Days 5, 10, 17, and 30. Mice were euthanized on Day 31. **B)** Graphical presentation of IVIS tumor burden from Day 5 to Day 31 as expressed as total flux in photons per second. Values are means +/- SD (n=8), one-way ANOVA with Tukey's multiple comparison test (* $p<0.05$). Experimental groups are: FAK-WT (blue boxes) control, FAK-WT plus CP (red boxes), FAK-NLS$^-$ (green boxes) control, and FAK-NLS$^-$ + CP (violet boxes). **C)** Experimental schematic similar as described in panel A with decreased amount of cisplatin (2 mg/kg) administered over a longer experimental time period. Mice were imaged at Day 5, randomized, and then received saline (control) or cisplatin over 40 days (CP on Day 10, 17, 24, 31, and 45). IVIS imaging performed on Day 5, 10, 17, 24, 31, 38, and 45). **D**) Representative IVIS images on FAK-WT-CP and FAK-NLS$^-$ CP mice on Day 45 with indicated heat map scale bar. **E)** Graphical presentation of IVIS tumor burden from Day 5 to Day 45. Experimental groups are: FAK-WT +CP (blue boxes) and FAK-NLS$^-$ + CP (red boxes). Values are means +/- SD (n=8), one-way ANOVA with Tukey's multiple comparison test (** $p<0.01$). **F)** Quantitation of total peritoneal cells recovered by IP saline wash after euthanasia by ViCell automated counting. FAK-WT +CP (blue circles) and FAK-NLS$^-$ + CP (red circles) are from individual mice and the mean is indicated by a line. Unpaired T test (* $P<0.05$).

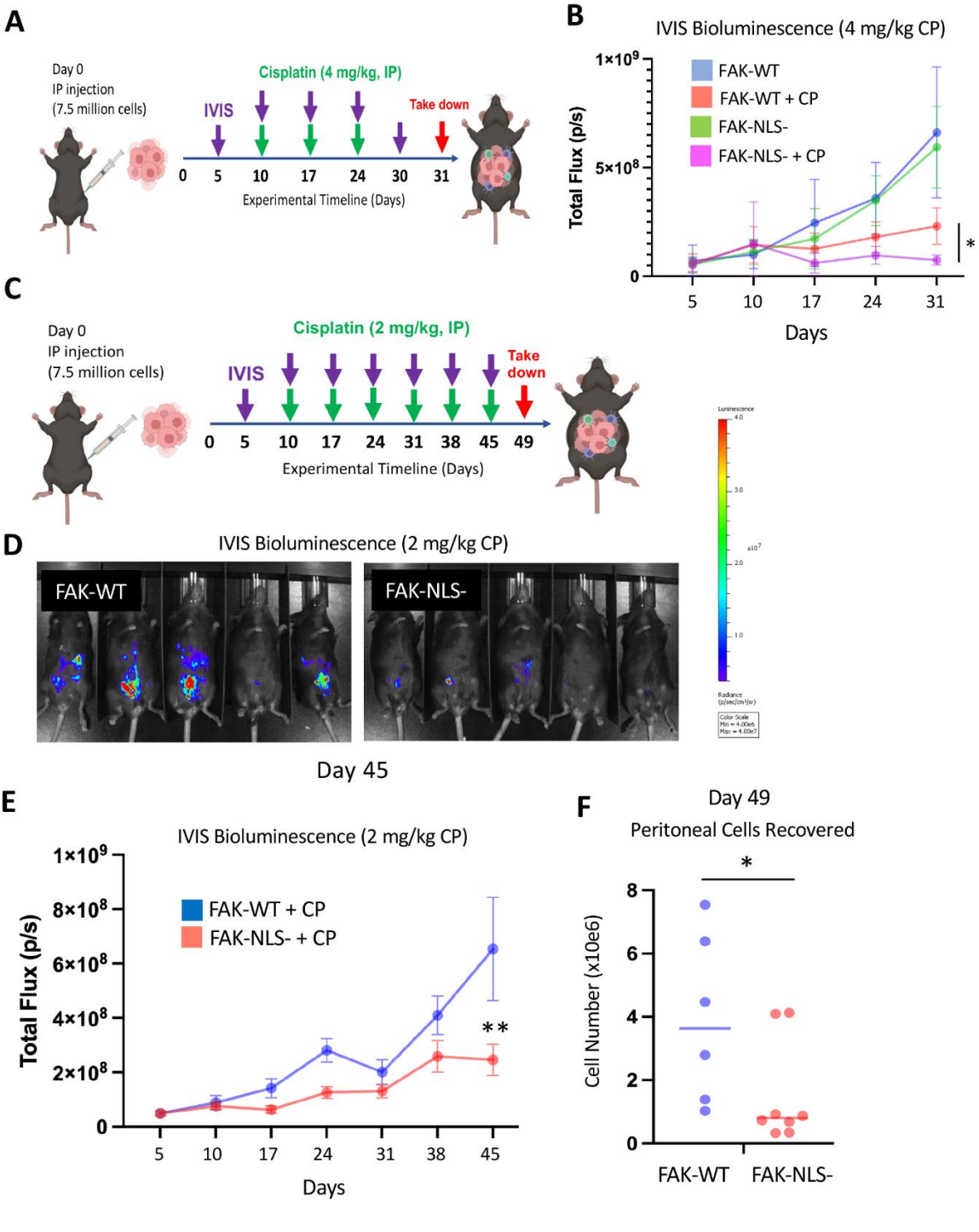

Zhang, Figure 3

MATERIALS AND METHODS

Cell Culture

Murine KMF cells were grown in Dulbecco's Modified Eagle Medium (DMEM, Gibco) Supplemented with 10% fetal bovine serum (FBS, Omega Scientific), 1 mM non-essential amino acids (Gibco), 100 µg/µL penicillin/streptomycin (Gibco). Human ovarian carcinoma OVCAR3, OVCAR4, and OVCAR10 cell lines were grown in Roswell Park Memorial Institute Medium (RPMI-1640, Gibco) containing 100 µg/µL penicillin/streptomycin (Gibco), 1 mM non-essential amino acids (Gibco), and 20% v/v FBS.

For virus transduction, we used both KMF FAK-knockout cells and OVCAR3 FAK-knockout cells and re-expressed with GFP fused WT FAK or GFP fused FAK NLS$^-$ lentivirus. 2x10^5 of KMF FAK-knockout cells or 5x10^5 OVCAR3 FAK-knockout cells were seeded as in 6 well plate overnight. 5 µl of 5 µg/ml of polybrene (Sigma-Aldrich: #H9268) were added onto each well with 5 µl of virus for each condition. Fresh mediums were changed after 24 hours. Cells were monitored and grew until a clear GFP signals can be seen under microscope (Discover Echo). For pChili-luciferase-labeled transductions, we used WT FAK re-expressed and NLS-FAK re-expressed cell from KMF FAK-knockout murine model. 2x10^5 of cells were seeded as in 6 well plate overnight. 5 µl of 5µg/ml of polybrene (Sigma-Aldrich: #H9268) were added onto each well with 1 ml of virus pChili-luciferase virus. Fresh mediums were changed after 24 hours. Cells were monitored and grew until a clear tdtomato signals can be seen under microscope (Discover Echo).

After virus transductions, 3x10^6 cells form each condition were sent to flow cytometry sorting for selecting either GFP-expressed cells or GFP-tdtomato doubled expressed cells. Flow cytometry sorting was performed by the flow core at The La Jolla Institute for Immunology.

Western blotting

If not specified below cells were plated, treated the next day (if applicable) and lysed at specified timepoints in RIPA buffer (Pierce). The nuclear and cytoplasmic fractionation was performed using NE-PER Nuclear and Cytoplasmic Extraction Reagents (Thermofisher, #78835). All protein lysis buffers were supplemented with Complete Mini ETDA-free Protease inhibitor cocktail and PhoSTOP phosphatase inhibitor cocktail (Roche Diagnostics). Twenty-five micrograms of total protein was used for immunoblotting. Total protein levels in lysates were determined through a bicinchoninic acid assay (Pierce), twenty-five micrograms of protein were resolved on Mini-Protean TGX Precast Gel (4–15% Tris/Glycine gel, Bio Rad, #456-1086), and transferred using a TransBlot Turbo (BioRad) and polyvinylidene difluoride (PDVF) membranes (Bio Rad) for subsequent immunoblotting. Levels of protein expression were detected by corresponding primary and secondary antibodies. The bands were visualized with Clarity Western ECL substrate (Bio Rad) reagent by chemiluminescence based reaction and blots were visualized with ChemiDoc Imaging System (BioRad).

Antibodies and reagents

Designation	Source or Reference	Additional Information
Anti-beta-Tubulin (Rabbit polyclonal)	Cell Signaling, Cat#2146S	WB (1:1000)
Anti-FAK (Mouse monoclonal)	Millipore Sigma, Clone4.47, Cat# 05-537	WB (1:1000)
Anti-phospho-FAK (Tyr397) (Rabbit monoclonal)	Abcam, clone EP2160Y; Cat# ab81298;	WB (1:1000)
Anti-Histone3 (Rabbit monoclonal)	Cell Signaling, Cat#4499S	WB (1:1000)
Anti-BAX (Rabbit polyclonal)	Cell Signaling, Cat 2722S	WB (1:1000)
Anti-Bcl2 (Rabbit monoclonal)	Cell Signaling, Cat 4223T	WB (1:1000)
Anti-Caspase 3 (Rabbit polyclonal)	Cell Signaling, Cat 9662S	WB (1:5000)
Anti-HA-tag (Mouse monoclonal)	Cell Signaling, Cat 2367S	WB (1:1000)
Cisplatin	West-ward Pharmaceuticals Inc. Cat 0143950401	
Paclitaxel	TEVA Pharmaceuticals, Cat 1384921	
Matrigel	Corning Cat 356255	

Colony formation assays

Cells were seeded (6000 cells/well) into 6-well plates. Control group was treated with 1 µl of DMSO and experimental groups were treated with increasing cisplatin concentration (0.1 and 10 µM). All groups grew in plates for 10 days. In the end of growth period, media was removed, cells were washed with PBS and fixed with cold ethanol. Cells were stained with 1% crystal violet solution for colony analysis. For statistical analysis, triplicate experimental points were evaluated, and experiments were repeated three times.

Viability and cytotoxicity

Cells were seeded (1x10^4 cells per well) in 96-well plates, after 24 hours increasing concentration of cisplatin was added to the plates. Cisplatin treatment lasted 48 hours, followed by incubation with Alamar Blue Reagent (Invitrogen, #2706294) for 4 hours at 37°C in 5% CO2 incubator according to manufacturer guidelines. Viability was then analyzed by detecting Absorbance at 570/600nm was read on SpectraMax ID3 plate reader and relative viability was calculated against control (0 µM Cisplatin) values. Plate assay included 3 technical replicates and were repeated three times, IC50 values were determined with Prism 8.0 software.

Mouse tumor growth

Mouse studies were performed in accordance with The Association for Assessment and Accreditation for Laboratory Animal Care guidelines and approved by the UCSD Institutional

Animal Care and Use Committee (protocol S07331). For GFP-FAK-WT or FAK-NLS⁻ tumor growth in mice, cells were harvested from culture, and 7.5x10^6 cells in 200 µl (50:50 serum free media plus Matrigel) were IP injected into peritoneum of 8 week-old female C57/Bl6 mice. Tumors were monitored using IVIS bioluminescent luciferase-based imaging system (Perkin Elmer) on indicated days. Mice were injected with luciferin intra-peritoneally (I.P.) and waited for 7 minutes before imaging. On day 5, after first indication of tumor implantation mice were randomized into treatment groups. Chemotherapy group received IP injections of cisplatin (2 mg/kg or 4 mg/kg) at designated days. Mice were euthanized by using 5 minutes of isoflurane and followed by cervical dislocation at indicated days. Peritoneal ascites was harvested by injecting 3 ml of PBS and collecting all peritoneal fluid. Overall, up to 8mL was collected. Red blood cells were removed (RBC lysis buffer, eBioscience, 00-4300-54), and remaining ascites cells were pelleted by centrifuge (1600 rpm for 6 min at 4°C). Cell pellets were resuspended in PBS and filtered through a 70 µm cell filter and single cells were counted.

Immunohistochemistry

For following GFP-FAK localization cells were seeded (3x10^5 cells/well) on coverslips in 6-well tissue culture plates, after initial 24-hour growth period, media was changed to media containing 20 µM of cisplatin. After 12 hr, coverslips were washed with PBS and fixed with 4% paraformaldehyde (Electron Microscopy Sciences, cat 15710-S) for 10 min at room temperature and permeabilized with 0.1% Triton X-100 (Thermofisher, # PI85111) for 15 mins at room temperature, followed blocking in 2%BSA in 1xPBS for 1 hour. The nuclei were counterstained

with DAPI (1 µg/ml) in blocking buffer for 10 mins. Coverslips were mounted on slides using antifading mounting medium (Vector Laboratories, H-1900). Images of GFP-FAK and nuclei were taken under Nikon Confocal Microscope with 40X oil magnification objectives settings, followed by protocols from Cancer Center Microscopy Shared Resource.

Statistics

Analyses were performed in Prism v8 (GraphPad Software). For experimental groups of three or more, statistical significance was calculated based on one-way ANOVA with Tukey's multiple comparison test. Unpaired T test was used to determine statistical difference between the means from two different samples. P values <0.05 were considered significant.

Funding

This work was funded by National Institutes of Health grants to D. Schlaepfer (R01CA24756 and R01CA254342).

REFERENCES

Agarwal, R., and S. B. Kaye. 2003. 'Ovarian cancer: strategies for overcoming resistance to chemotherapy', *Nat Rev Cancer*, 3: 502-16.

Albasri, A., W. Fadhil, J. H. Scholefield, L. G. Durrant, and M. Ilyas. 2014. 'Nuclear expression of phosphorylated focal adhesion kinase is associated with poor prognosis in human colorectal cancer', *Anticancer Res*, 34: 3969-74.

Bowtell, D. D., S. Bohm, A. A. Ahmed, P. J. Aspuria, R. C. Bast, Jr., V. Beral, J. S. Berek, M. J. Birrer, S. Blagden, M. A. Bookman, J. D. Brenton, K. B. Chiappinelli, F. C. Martins, G. Coukos, R. Drapkin, R. Edmondson, C. Fotopoulou, H. Gabra, J. Galon, C. Gourley, V. Heong, D. G. Huntsman, M. Iwanicki, B. Y. Karlan, A. Kaye, E. Lengyel, D. A. Levine, K. H. Lu, I. A. McNeish, U. Menon, S. A. Narod, B. H. Nelson, K. P. Nephew, P. Pharoah, D. J. Powell, Jr., P. Ramos, I. L. Romero, C. L. Scott, A. K. Sood, E. A. Stronach, and F. R. Balkwill. 2015. 'Rethinking ovarian cancer II: reducing mortality from high-grade serous ovarian cancer', *Nat Rev Cancer*, 15: 668-79.

Byeon, Y., J. W. Lee, W. S. Choi, J. E. Won, G. H. Kim, M. G. Kim, T. I. Wi, J. M. Lee, T. H. Kang, I. D. Jung, Y. J. Cho, H. J. Ahn, B. C. Shin, Y. J. Lee, A. K. Sood, H. D. Han, and Y. M. Park. 2018. 'CD44-Targeting PLGA Nanoparticles Incorporating Paclitaxel and FAK siRNA Overcome Chemoresistance in Epithelial Ovarian Cancer', *Cancer Res*, 78: 6247-56.

Cai, X., D. Lietha, D. F. Ceccarelli, A. V. Karginov, Z. Rajfur, K. Jacobson, K. M. Hahn, M. J. Eck, and M. D. Schaller. 2008. 'Spatial and temporal regulation of focal adhesion kinase activity in living cells', *Mol Cell Biol*, 28: 201-14.

Canel, M., A. Byron, A. H. Sims, J. Cartier, H. Patel, M. C. Frame, V. G. Brunton, B. Serrels, and A. Serrels. 2017. 'Nuclear FAK and Runx1 Cooperate to Regulate IGFBP3, Cell-Cycle Progression, and Tumor Growth', *Cancer Res*, 77: 5301-12.

Ceccarelli, D. F., H. K. Song, F. Poy, M. D. Schaller, and M. J. Eck. 2006. 'Crystal structure of the FERM domain of focal adhesion kinase', *J Biol Chem*, 281: 252-9.

Chen, X. L., J. O. Nam, C. Jean, C. Lawson, C. T. Walsh, E. Goka, S. T. Lim, A. Tomar, I. Tancioni, S. Uryu, J. L. Guan, L. M. Acevedo, S. M. Weis, D. A. Cheresh, and D. D. Schlaepfer. 2012. 'VEGF-induced vascular permeability is mediated by FAK', *Dev Cell*, 22: 146-57.

Dawson, J. C., A. Serrels, D. G. Stupack, D. D. Schlaepfer, and M. C. Frame. 2021. 'Targeting FAK in anticancer combination therapies', *Nat Rev Cancer*, 21: 313-24.

Diaz Osterman, C. J., D. Ozmadenci, E. G. Kleinschmidt, K. N. Taylor, A. M. Barrie, S. Jiang, L. M. Bean, F. J. Sulzmaier, C. Jean, I. Tancioni, K. Anderson, S. Uryu, E. A. Cordasco, J. Li, X. L. Chen, G. Fu, M. Ojalill, P. Rappu, J. Heino, A. M. Mark, G. Xu, K. M. Fisch, V. N. Kolev, D. T. Weaver, J. A. Pachter, B. Gyorffy, M. T. McHale, D. C. Connolly, A. Molinolo, D. G. Stupack, and D. D. Schlaepfer. 2019. 'FAK activity sustains intrinsic and acquired ovarian cancer resistance to platinum chemotherapy', *Elife*, 8: 10.7554/eLife.47327.

Dunty, J. M., V. Gabarra-Niecko, M. L. King, D. F. Ceccarelli, M. J. Eck, and M. D. Schaller. 2004. 'FERM domain interaction promotes FAK signaling', *Mol Cell Biol*, 24: 5353-68.

Halder, J., C. N. Landen, Jr., S. K. Lutgendorf, Y. Li, N. B. Jennings, D. Fan, G. M. Nelkin, R. Schmandt, M. D. Schaller, and A. K. Sood. 2005. 'Focal adhesion kinase silencing augments docetaxel-mediated apoptosis in ovarian cancer cells', *Clin Cancer Res*, 11: 8829-36.

Jeong, K., J. H. Kim, J. M. Murphy, H. Park, S. J. Kim, Y. A. R. Rodriguez, H. Kong, C. Choi, J. L. Guan, J. M. Taylor, T. M. Lincoln, W. T. Gerthoffer, J. S. Kim, E. E. Ahn, D. D. Schlaepfer, and S. S. Lim. 2019. 'Nuclear Focal Adhesion Kinase Controls Vascular Smooth Muscle Cell Proliferation and Neointimal Hyperplasia Through GATA4-Mediated Cyclin D1 Transcription', *Circ Res*, 125: 152-66.

Jeong, K., J. M. Murphy, E. E. Ahn, and S. S. Lim. 2022. 'FAK in the nucleus prevents VSMC proliferation by promoting p27 and p21 expression via Skp2 degradation', *Cardiovasc Res*, 118: 1150-63.

Kang, Y., W. Hu, C. Ivan, H. J. Dalton, T. Miyake, C. V. Pecot, B. Zand, T. Liu, J. Huang, N. B. Jennings, R. Rupaimoole, M. Taylor, S. Pradeep, S. Y. Wu, C. Lu, Y. Wen, J. Huang, J. Liu, and A. K. Sood. 2013. 'Role of focal adhesion kinase in regulating YB-1-mediated paclitaxel resistance in ovarian cancer', *J Natl Cancer Inst*, 105: 1485-95.

Kang, Y., A. S. Nagaraja, G. N. Armaiz-Pena, P. L. Dorniak, W. Hu, R. Rupaimoole, T. Liu, K. M. Gharpure, R. A. Previs, J. M. Hansen, C. Rodriguez-Aguayo, C. Ivan, P. Ram, V. Sehgal, G. Lopez-Berestein, S. K. Lutgendorf, S. W. Cole, and A. K. Sood. 2016. 'Adrenergic Stimulation of DUSP1 Impairs Chemotherapy Response in Ovarian Cancer', *Clin Cancer Res*, 22: 1713-24.

Kaveh, F., L. O. Baumbusch, D. Nebdal, A. L. Borresen-Dale, O. C. Lingjaerde, H. Edvardsen, V. N. Kristensen, and H. K. Solvang. 2016. 'A systematic comparison of copy number alterations in four types of female cancer', *BMC Cancer*, 16: 913.

Kim, S., Y. Han, S. I. Kim, H. S. Kim, S. J. Kim, and Y. S. Song. 2018. 'Tumor evolution and chemoresistance in ovarian cancer', *NPJ Precis Oncol*, 2: 20.

Lietha, D., X. Cai, D. F. Ceccarelli, Y. Li, M. D. Schaller, and M. J. Eck. 2007. 'Structural basis for the autoinhibition of focal adhesion kinase', *Cell*, 129: 1177-87.

Lim, S. T., X. L. Chen, Y. Lim, D. A. Hanson, T. T. Vo, K. Howerton, N. Larocque, S. J. Fisher, D. D. Schlaepfer, and D. Ilic. 2008. 'Nuclear FAK promotes cell proliferation and survival through FERM-enhanced p53 degradation', *Mol Cell*, 29: 9-22.

Lim, S. T., N. L. Miller, X. L. Chen, I. Tancioni, C. T. Walsh, C. Lawson, S. Uryu, S. M. Weis, D. A. Cheresh, and D. D. Schlaepfer. 2012. 'Nuclear-localized focal adhesion kinase regulates inflammatory VCAM-1 expression', *J Cell Biol*, 197: 907-19.

Matulonis, U. A., A. K. Sood, L. Fallowfield, B. E. Howitt, J. Sehouli, and B. Y. Karlan. 2016. 'Ovarian cancer', *Nat Rev Dis Primers*, 2: 16061.

Mitra, S. K., D. A. Hanson, and D. D. Schlaepfer. 2005. 'Focal adhesion kinase: in command and control of cell motility', *Nat Rev Mol Cell Biol*, 6: 56-68.

Murphy, J. M., Y. A. R. Rodriguez, K. Jeong, E. E. Ahn, and S. S. Lim. 2020. 'Targeting focal adhesion kinase in cancer cells and the tumor microenvironment', *Exp Mol Med*, 52: 877-86.

Patel, M. R., J. R. Infante, K. N. Moore, M. Keegan, A. Poli, M. Padval, S. F. Jones, J. Horobin, and H. A. Burris. 2014. 'Phase I/Ib study of the FAK inhibitor defactinib (VS-6063) in combination with weekly paclitaxel for advanced ovarian cancer.', *ASCO Annual Meeting Abstracts*, 32: 5521.

Pereira, L., A. Igea, B. Canovas, I. Dolado, and A. R. Nebreda. 2013. 'Inhibition of p38 MAPK sensitizes tumour cells to cisplatin-induced apoptosis mediated by reactive oxygen species and JNK', *EMBO Mol Med*, 5: 1759-74.

Schlaepfer, D. D., C. R. Hauck, and D. J. Sieg. 1999. 'Signaling through focal adhesion kinase', *Prog Biophys Mol Biol*, 71: 435-78.

Serrels, A., T. Lund, B. Serrels, A. Byron, R. C. McPherson, A. von Kriegsheim, L. Gomez-Cuadrado, M. Canel, M. Muir, J. E. Ring, E. Maniati, A. H. Sims, J. A. Pachter, V. G. Brunton, N. Gilbert, S. M. Anderton, R. J. Nibbs, and M. C. Frame. 2015. 'Nuclear FAK controls chemokine transcription, Tregs, and evasion of anti-tumor immunity', *Cell*, 163: 160-73.

Siegel, R. L., K. D. Miller, N. S. Wagle, and A. Jemal. 2023. 'Cancer statistics, 2023', *CA Cancer J Clin*, 73: 17-48.

Sulzmaier, F. J., C. Jean, and D. D. Schlaepfer. 2014. 'FAK in cancer: mechanistic findings and clinical applications', *Nat Rev Cancer*, 14: 598-610.

Tancioni, I., N. L. Miller, S. Uryu, C. Lawson, C. Jean, X. L. Chen, E. G. Kleinschmidt, and D. D. Schlaepfer. 2015. 'FAK activity protects nucleostemin in facilitating breast cancer spheroid and tumor growth', *Breast Cancer Res*, 17: 47.

Tancioni, I., S. Uryu, F. J. Sulzmaier, N. R. Shah, C. Lawson, N. L. Miller, C. Jean, X. L. Chen, K. K. Ward, and D. D. Schlaepfer. 2014. 'FAK Inhibition disrupts a beta5 integrin signaling axis controlling anchorage-independent ovarian carcinoma growth', *Mol Cancer Ther*, 13: 2050-61.

Ward, K. K., I. Tancioni, C. Lawson, N. L. Miller, C. Jean, X. L. Chen, S. Uryu, J. Kim, D. Tarin, D. G. Stupack, S. C. Plaxe, and D. D. Schlaepfer. 2013. 'Inhibition of focal adhesion kinase (FAK) activity prevents anchorage-independent ovarian carcinoma cell growth and tumor progression', *Clin Exp Metastasis*, 30: 579-94.

Xu, B., J. Lefringhouse, Z. Liu, D. West, L. A. Baldwin, C. Ou, L. Chen, D. Napier, L. Chaiswing, L. D. Brewer, D. St Clair, O. Thibault, J. R. van Nagell, B. P. Zhou, R. Drapkin, J. A. Huang, M. L. Lu, F. R. Ueland, and X. H. Yang. 2017. 'Inhibition of the integrin/FAK signaling axis and c-Myc synergistically disrupts ovarian cancer malignancy', *Oncogenesis*, 6: e295.